PAPER Special Section on Recent Progress in Antennas and Propagation in Conjunction with Main Topics of ISAP2010

Proper Derivation of Equivalent-Circuit Expressions of Intra-Body Communication Channels Using Quasi-Static Field

Nozomi HAGA[†a)], ***Student Member***, **Kazuyuki SAITO**[††], ***Member***, **Masaharu TAKAHASHI**[††], ***Senior Member***, ***and*** **Koichi ITO**[†], ***Fellow***

SUMMARY Physical channels of the intra-body communications, in which communications are performed by exciting electric field around the human body, have been treated as a capacitive circuit from the beginning of the development. Although the circuit-like understanding of the channels are helpful to design devices and systems, there is a problem that the results may be invalid if the circuit parameters are incorrectly estimated. In the present study, the values of the circuit parameters are properly derived by solving a boundary value problem of electric potentials of the conductors. Furthermore, approximate models which are appropriate for cases that some of the conductors are grounded are investigated.

key words: *intra-body communications, quasi-static approximation, equivalent circuit, boundary value problem*

1. Introduction

In recent years, body-centric communications, by which wireless networks are composed between wearable devices, have become an active area of research because of their various applications such as e-healthcare, security systems, and personal services [1]–[11]. The body-centric communications using electric field below several megahertz around the human body are also known as intra-body communications. The physical channels of the intra-body communications have been treated as a capacitive circuit since it was firstly devised by Zimmerman in 1995 [4]–[7]. In the beginning, the human body was modeled by a perfect conductor [4]. Afterward, loss and voltage drop due to conduction currents inside the human body was taken into account by introducing a distributed *RC* circuit model; and its validity was examined by experiments [6]. These circuit-like understandings of the channels are helpful to design devices and systems; however, there is a problem that the results may be invalid if the circuit parameters are incorrectly estimated. Moreover, applicable scopes of these circuit models are still unclear. For instance, in [6], the transmitted signals were received by earth-grounded instruments such as a spectrum analyzer and an oscilloscope. Therefore, there is no proof that the model may be applied for cases that the receiver is not grounded or only the transmitter is grounded.

Meanwhile, analyses as an antenna excitation problem were widely conducted by using full-wave analysis methods such as the finite-difference time-domain (FDTD) method and the method of moment (MoM) [9]–[11]. These approaches have advantages as below: they can be flexibly applied for cases that the wave length is comparable with the dimensions of human body; they bring correct results as far as the analytical precision is ensured. However, there is a drawback that it is difficult to clearly understand the obtained results as a physical phenomenon.

Therefore, it is necessary to correctly know the composition of the equivalent-circuit model and the concrete values of respective parameters. In the present study, the values of the circuit parameters are properly derived by solving a boundary value problem of electric potentials of the electrodes and the human body. Furthermore, approximate models which are appropriate for cases that some of the conductors are grounded are investigated. For example, a case that the body is grounded corresponds to a situation that the user stands on the earth barefoot. Other cases that either or both of the transmitter and the receiver are grounded correspond to various kinds of off-body applications, including personal authentication, electronic payment, and so forth. These investigations will clarify the validity and applicable scope of the previously-proposed equivalent circuit models. The approach of the present study can be applied only for the low frequency range in which the wavelength is much longer than the human body and conduction currents inside the body are ignorable. For example, the frequency should be much less than 70 MHz, at which half-wavelength is comparable with the height of the human body. Nevertheless, the results of the present study will be useful to design and assess the devices and the systems because they are based on an electrostatically-proper analysis.

2. Procedure to Derive the Equivalent Circuit

First of all, we describe the procedure to express the general problem of conductor systems as an equivalent circuit. As an example, in a case that three conductors are in free space as shown in Fig. 1(a), the potentials and the net charges of respective conductors have a linear relationship as below.

$$\begin{pmatrix} c_{11} & c_{12} & c_{13} \\ c_{21} & c_{22} & c_{23} \\ c_{31} & c_{32} & c_{33} \end{pmatrix} \begin{pmatrix} \phi_1 \\ \phi_2 \\ \phi_3 \end{pmatrix} = \begin{pmatrix} q_1 \\ q_2 \\ q_3 \end{pmatrix} \tag{1}$$

where, c_{ij} is the capacitance coefficient, ϕ_j is the potential

Manuscript received March 7, 2011.
Manuscript revised July 12, 2011.

[†]The author is with the Graduate School of Engineering, Chiba University, Chiba-shi, 263-8522 Japan.
[††]The author is with the Reserch Center for Frontier Medical Enginnering, Chiba University, Chiba-shi, 263-8522 Japan.
a) E-mail: n_haga@graduate.chiba-u.jp

DOI: 10.1587/transcom.E95.B.51

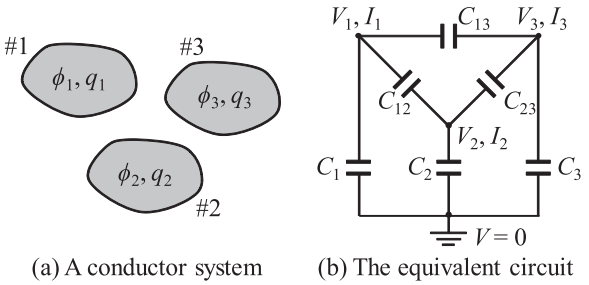

Fig. 1 An example of multiple conductor systems and the corresponding equivalent circuit expression.

of each conductor, and q_i is the net charge. Each capacitance coefficient can be obtained by solving a boundary value problem of electric potentials of the conductors. For example, by obtaining the charge distributions of each conductor under a condition of $\boldsymbol{\phi} = (1, 0, 0)^T$, we can find the values as $c_{11} = q_1$, $c_{21} = q_2$, and $c_{31} = q_3$. The potentials of each conductor in arbitrary net charge conditions can be obtained by solving Eq. (1) in which the charge vector in the right hand is specified.

Figure 1(b) shows the equivalent circuit corresponding to the conductor system. This circuit is a network of which all nodes including the infinite distance of reference potential ($V = 0$) are connected with capacitors. The nodal equation of the circuit is as follows.

$$j\omega \begin{pmatrix} C_1+C_{12}+C_{13} & -C_{12} & -C_{13} \\ -C_{12} & C_2+C_{12}+C_{23} & -C_{23} \\ -C_{13} & -C_{23} & C_3+C_{13}+C_{23} \end{pmatrix} \begin{pmatrix} V_1 \\ V_2 \\ V_3 \end{pmatrix} = \begin{pmatrix} I_1 \\ I_2 \\ I_3 \end{pmatrix} = j\omega \begin{pmatrix} Q_1 \\ Q_2 \\ Q_3 \end{pmatrix} \tag{2}$$

where, V_j is the potential of each node, I_i is the current flowing into each node. Considering the relationship of $I = j\omega Q$ between current I and charge Q, we find that the relationship of Eq. (2) is essentially equal to that of Eq. (1). Hence, by comparing these matrices, the equivalent-circuit parameters can be formally obtained as $C_1 = c_{11} + c_{12} + c_{13}$, $C_{12} = -c_{12}$, and $C_{13} = -c_{13}$.

3. Model and Numerical Methods for Investigation

Figure 2 shows the structure of the model for the present investigation. For simplicity, the human body is modeled by a perfect conducting sphere. Its diameter is 300 mm which corresponds to the longest diameter of the human torso [12]. The transmitter and the receiver have a same structure of which two electrodes are 30 mm in side length and separated each other by a gap of 5 mm. These dimensions are small enough both for on- and off-body applications. Both of the transmitter and the receiver are equipped on the conducting sphere with a 5-mm separation from the sphere, assuming some covers and clothes. The angle θ formed between the transmitter and the receiver is varied from 20° to 180°. Incidentally, since the actual human body has some amount

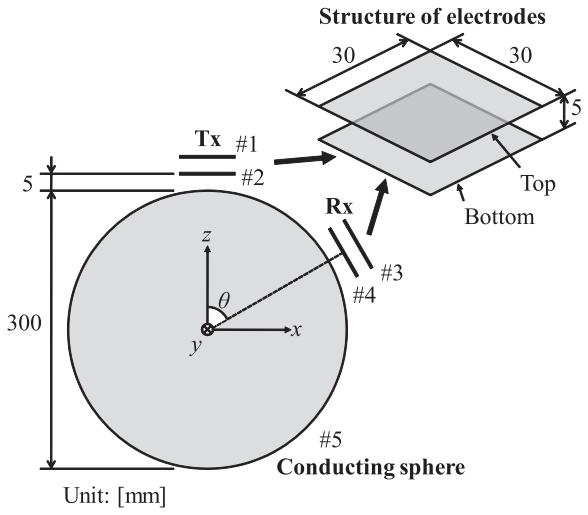

Fig. 2 Model for the investigation.

of resistance, the voltage drop and the loss due to conducting currents inside the body are expected to get larger as the frequency increases. Regarding to this, we have already conducted some additional tests and confirmed that the discrepancy of received voltage from the static approximation is at most 3 dB in a range below 60 MHz. The detail is described in the Appendix.

The static characteristics of the model were numerically analyzed by using the method of moment (MoM) based on the potential integral equation and the Galerkin's method [13]. The electrodes are divided into rectangular constant elements which have unit net charge. The ratio of the mesh sizes is equal to that of weight factors for the Gaussian quadrature [14]; that is, the meshes neighboring the edges have the minimum size. Division number of each electrode is 32×32. Instead of dividing the sphere into elements, we used a Green's function of which value is zero on the surface of the sphere. This Green's function is based on the image charge method [15], and transformed to a reciprocal form between the source and observation points as follows.

$$G(\boldsymbol{r}, \boldsymbol{r}') = \frac{1}{|\boldsymbol{r} - \boldsymbol{r}'|} - \frac{1}{\sqrt{|\boldsymbol{r}|^2|\boldsymbol{r}'|^2/a^2 - 2\boldsymbol{r} \cdot \boldsymbol{r}' + a^2}} \tag{3}$$

where, $\boldsymbol{r}$ is the observation point, $\boldsymbol{r}'$ is the source point, and a is the radius of the sphere. If the given potential on the sphere ϕ_{sphere} is not zero, a point charge can be assumed at the center of the sphere so as to satisfy the given boundary condition. Therefore, the integral equation to be solved is as follows.

$$\phi(\boldsymbol{r}) - \frac{a}{|\boldsymbol{r}|}\phi_{\text{sphere}} = \frac{1}{4\pi\epsilon_0} \int_S G(\boldsymbol{r}, \boldsymbol{r}')\sigma(\boldsymbol{r}')dS' \tag{4}$$

where, the second term of the left hand is the contribution of the point charge, ϵ_0 is the permittivity of vacuum, σ is the surface charge on the electrodes, and S is the surface region of the electrodes.

In order to validate the MoM analysis described above, we also employed the FDTD method. The dimensions of the computational domain are 600 mm × 600 mm × 600 mm; and 20-layer perfectly matched layer (PML) surrounds the domain. The cell sizes in a region including the electrodes and the sphere are $\Delta x = \Delta y = \Delta z = 1$ mm. The sphere is approximated by using the staircasing. The maximum cell size neighboring the PML absorbing boundary is 5 mm. The transmitter is fed at the central point of the electrodes by a current source with uniform current distributions and infinite internal impedance. The exciting waveform is the derivative Gaussian pulse, of which spectrum is −60 dB at 1 GHz. Since the feeding charge is a time integral of the feeding current, the charge has a waveform of the Gaussian pulse; therefore, the spectrum of the charge has maximum value at zero frequency. The top and bottom electrodes of the receiver are open ended in order to obtain open voltages by a line integral of the electric field.

As well as in the MoM analysis, the static characteristics should be obtained in this FDTD analysis. In the present case, the number of the PML layers is large enough so that its precision is ensured for relatively-low frequency [16]. Thus, the convergence of the field of interest is faster than the risetime of the undesired reflections from corners of outer boundaries. For this reason, by terminating the iterative updates of electromagnetic field and the Fourier transform immediately after the convergence of field, the static characteristics can be obtained with acceptable accuracy. The duration of the filed calculation is about 19.2–57.6 ns, depending on cases. The time of the convergence were confirmed by once observing the long-duration transient field at a corner of the domain. Then, the field distributions were calculated again in a shorter duration appropriate for each case. Incidentally, if the number of the PML layers is not enough, the risetime of the undesired reflections is much faster, and so they are unable to be excluded. Likewise, if the maximum frequency of the exciting pulse is too lower, the time for the convergence is much longer; therefore, the field of interest is unable to be separated with the reflections. We have figured out enough values for the pulse waveform and the PML layers through trial-and-error processes.

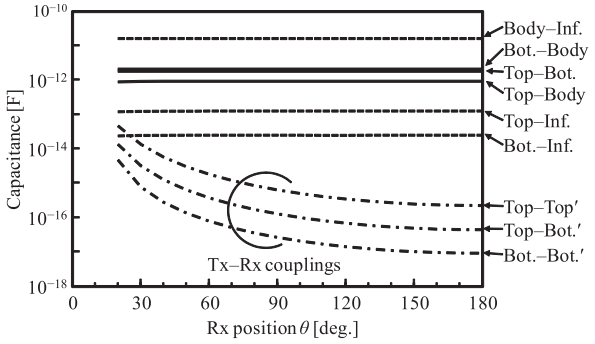

Fig. 3 Calculated equivalent-circuit parameters.

Table 1 Numerical values of equivalent-circuit parameters.

Parameter	$\theta = 90°$	$\theta = 180°$
Body–Inf.	1.642×10^{-11}	1.642×10^{-11}
Bot.–Body	2.121×10^{-12}	2.121×10^{-12}
Top–Bot.	1.774×10^{-12}	1.774×10^{-12}
Top–Body	9.138×10^{-13}	9.143×10^{-13}
Top–Inf.	1.221×10^{-13}	1.221×10^{-13}
Bot.–Inf.	2.424×10^{-14}	2.419×10^{-14}
Top–Top′	6.355×10^{-16}	2.239×10^{-16}
Top–Bot.′	1.286×10^{-16}	4.478×10^{-17}
Bot.–Bot.′	2.602×10^{-17}	8.966×10^{-18}

Unit: [F]

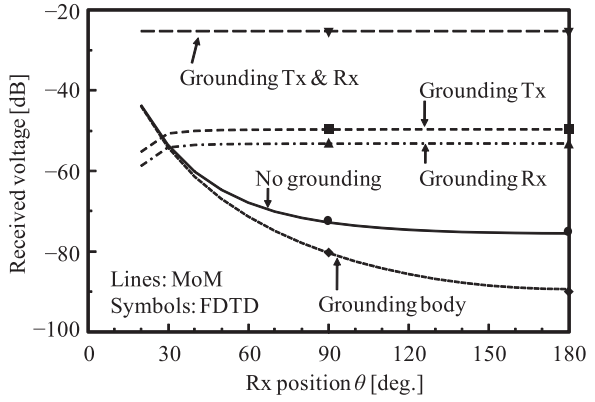

Fig. 4 Received voltages in various conditions.

4. Parameters of Equivalent Circuit and Signal Transmission Characteristics

Figure 3 plots the equivalent-circuit parameters calculated by the MoM. The solid lines indicate the capacitances between the electrodes of one device and the body (Bot.–Body, Top–Bot., and Top–Body); the broken lines indicate the capacitances of each conductor with the infinite distance (Body–Inf., Top–Inf., and Bot.–Inf.); and the chained line indicate the capacitances between respective electrodes of the transmitter and the receiver (Top–Top′, Top–Bot.′, and Bot.–Bot.′: Tx–Rx couplings). In addition, specific values of the parameters at $\theta = 90°$ and 180° are listed in Table 1. Naturally, the direct couplings between the transmitter and the receiver depend on the receiver position θ; and their values are relatively small compared with the others. By contrast, the other parameters hardly depend on θ; and the largest one is the capacitance of the body with the infinite distance (Body–Inf.), followed by that between each conductor (Bot.–Body, Top–Bot., and Top–Body), and that of each electrode with the infinite distance (Top–Inf. and Bot.–Inf.). The large amount of the capacitance of the body with the infinite distance is due to the large dimension of the body.

Figure 4 plots the received voltages in various conditions. Here the received voltages are normalized by the input voltage. In the case that no conductor is grounded (No grounding: this case corresponds to some on-body applications such as sensing of biological information and head mount displays [1], [3]), the received voltage decreases with

increasing θ. This fact indicates that the direct couplings between the transmitter and the receiver are not negligible even though their values are relatively small; and accordingly, the equipping position of devices and user's postures are important for the on-body applications. At large θ more than about 120°, however, the received voltage almost converges; that is, contribution of the direct couplings becomes relatively small. By contrast, when the body is grounded (Grounding body), the received voltage does not converge even at large θ. This is due to a fact that the coupling through the infinite distance is not available because the body and the infinite distance are equal in potential as also described in [4]. In the cases that the top electrode of one device is grounded (Grounding Tx and Grounding Rx), the value and the stability of the received voltage are considerably improved. This is because the coupling through the infinite distance is dominant. These results suggest that the equipping position of devices is not so important in the off-body applications. Furthermore, when the both devices are grounded, the performance is better than the previous cases. Incidentally, the symbols plotted in Fig. 4 indicate the results by the FDTD method. In order to ground some conductors, thin conducting wires are connected with them and extended into inside of the PML. Therefore, the models for the FDTD and the MoM are not exactly the same; however, the calculated values almost agree with each other. Hence, the numerical analyses conducted here are most likely valid.

In addition, in order to understand the phenomenon from electromagnetic view, Figs. 5(a)–(e) shows the electric field distributions on the plane of $y = 0$ when $\theta = 180°$ in respective cases. In all the cases, the distributions by the MoM and the FDTD agree with each other, as well as in Fig. 4. Comparing (b) to (a), the distributions around the transmitter (top side of the sphere) are almost the same as that in (a), but attenuate more rapidly. That is because the electric charges which contribute to the electric field around the bottom side in (a) have gone away to the infinite distance (or the earth ground).

Regarding (c), the distributions are almost uniform around the surface of the sphere. This corresponds to the stability of the received voltage in Fig. 4, and is because the absolute value of the potential of the sphere (contributed by the point charge assumed at the center of the sphere) is larger than that in (a). On the other hand, the distributions in (d) are not uniform as in (c). But since the potential should be constant on the sphere and that of the grounded electrode is forced to be zero, the potential difference between them is also constant; therefore, almost uniform electric field is supposed to be generated between them. Actually, as shown in (d), the electric field in a region between the body and the grounded electrode seems to be enhanced. In another respect, this is contributed by charges supplied from the infinite distance to the grounded electrodes. This is the alternative proof that the received voltage is stable when the receiver is grounded.

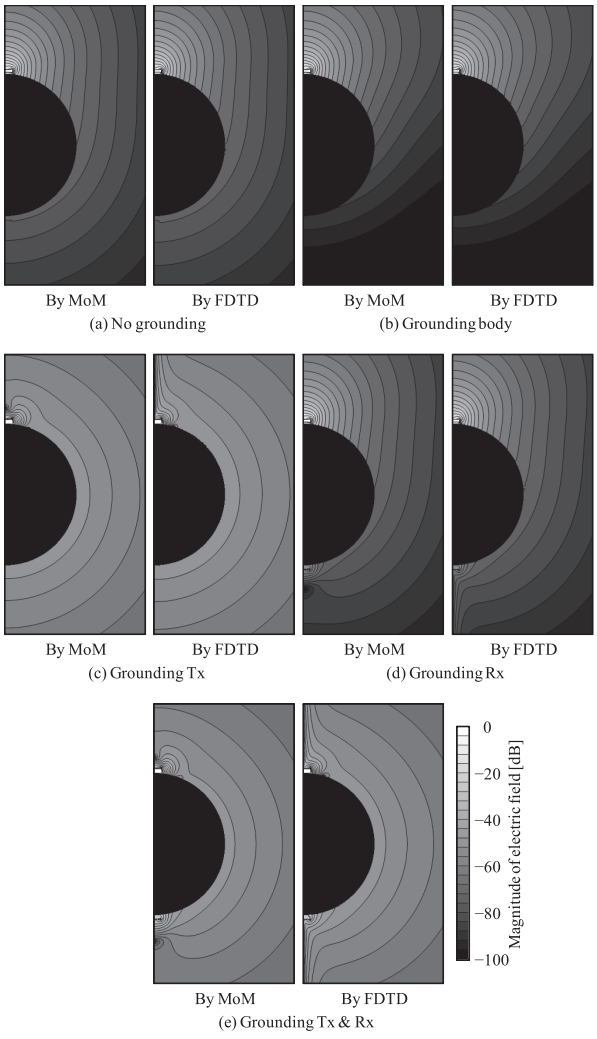

Fig. 5 Electric field distributions in various conditions.

5. Investigations of Approximate Circuit Models

In this section, we select negligible parameters out in each case considered in the previous section, and investigate what approximate models are reasonable.

5.1 Case 1: No Conductor is Grounded

In order to figure important parameters out first, Fig. 6 plots the received voltages with omitting some parameters in the case that no conductor is grounded. First, the received voltage with omitting the direct couplings between the transmitter and the receiver is quite different from the exact one as already suggested in the previous section (Omit. Tx–Rx). But another result with omitting the direct coupling only between the bottom electrodes agrees with the exact result (Omit. Bot.–Bot.′); and furthermore, even if only the direct coupling between the top electrodes is taken into account, the result largely agrees with the exact one (Omit. Tx–Rx except Top–Top′).

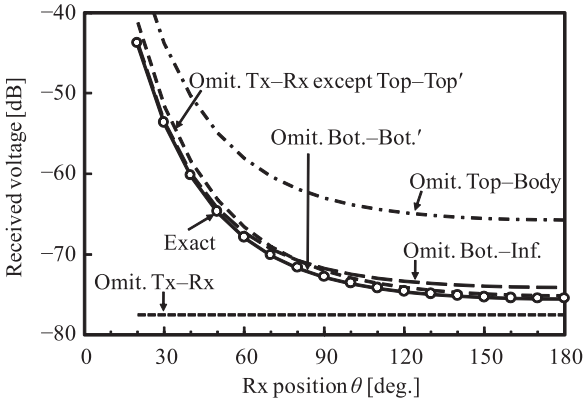

Fig. 6 Received voltages with omitting some parameters when no conductor grounded.

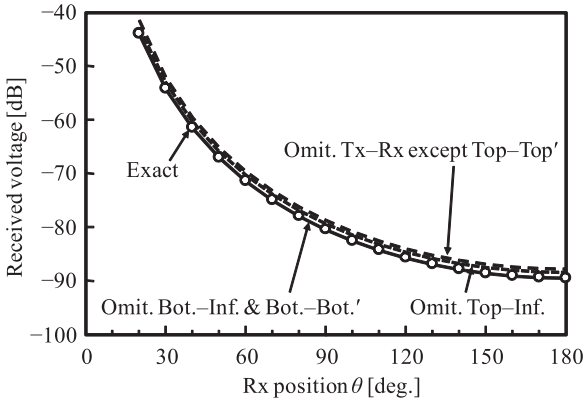

Fig. 8 Received voltages with omitting some parameters when the body is grounded.

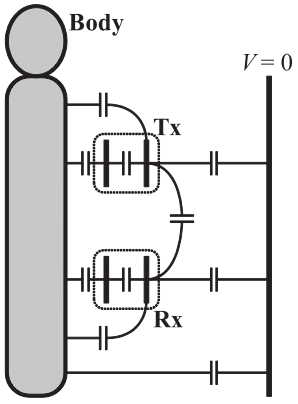

Fig. 7 Approximate model when no conductor is grounded.

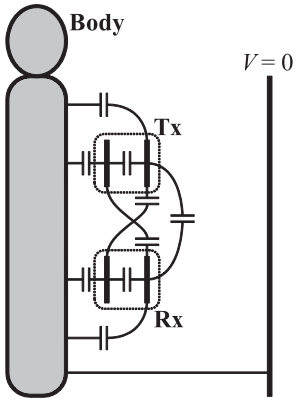

Fig. 9 Approximate model when the body is grounded.

Regarding other parameters, in the case that the coupling between each top electrode and the human body is omitted, the estimated received voltage is almost 10 dB higher than the exact one (Omit. Top–Body); therefore, it is not omissible. Finally, the result with omitting the coupling between each bottom electrode and the infinite distance has a little discrepancy with the exact one at larger θ (Omit. Bot.–Inf.); but the amount is less than 1.4 dB. Considering these results, it is concluded that at least parameters shown in Fig. 7 should be taken into account. The model in Fig. 7 is much more complicated than any other approximate models proposed previously. In addition, we would like to note again that the direct coupling between the transmitter and the receiver is significant in the on-body applications and the equipping position and user's posture should be taken into account.

5.2 Case 2: The Body is Grounded

Next, we discuss the case that the human body is grounded. In this case, the human body and the infinite distance are equal in potential; therefore, capacitances of each electrode with the reference potential are the sum of those with the human body and with the infinite distance. Since the capacitances with the human body are sufficiently larger than those with the infinite distance, the capacitances of each conductor with the infinite distance are expected to be omissible. Figure 8 plots the received voltages with omitting some parameters. In the case that the capacitance of the bottom electrodes with the infinite distance and that between each bottom electrode, the result almost agrees with the exact one (Omit. Bot.–Inf. & Bot.–Bot.′). On the other hand, the result with omitting capacitances of each top electrode with the infinite distance do not exactly agree with the exact one (Omit. Top–Inf.). However, the discrepancy is less than 1.1 dB; therefore, they are most likely omissible. In addition, in the case that the direct couplings between the transmitter and the receiver except between the top electrodes are omitted, the discrepancy is somewhat larger (1.7 dB) than that in the ungrounded case. According to these results, the approximate circuit model for this case is as shown in Fig. 9.

5.3 Case 3: Devices are Grounded

Finally, we consider the cases that either or both of the transmitter and the receiver are grounded. If one device is grounded, the capacitances between the electrodes of other device and the reference potential are the sum of those with the grounded electrode and with the infinite distance. Since the direct couplings between the transmitter and the re-

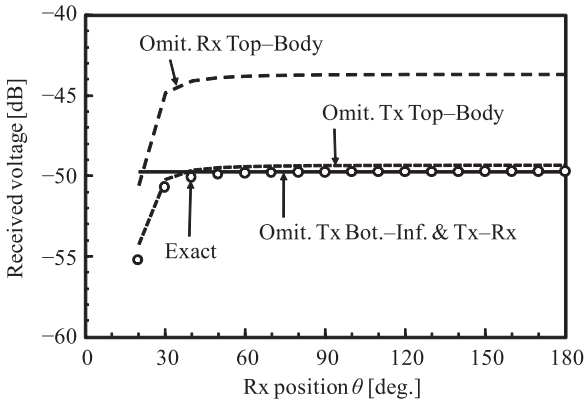

Fig. 10 Received voltages with omitting some parameters when the transmitter is grounded.

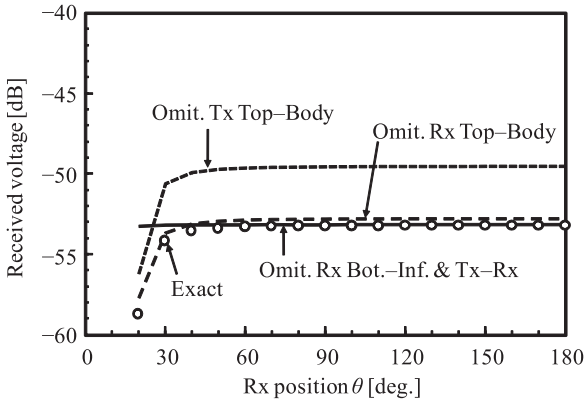

Fig. 11 Received voltages with omitting some parameters when the receiver is grounded.

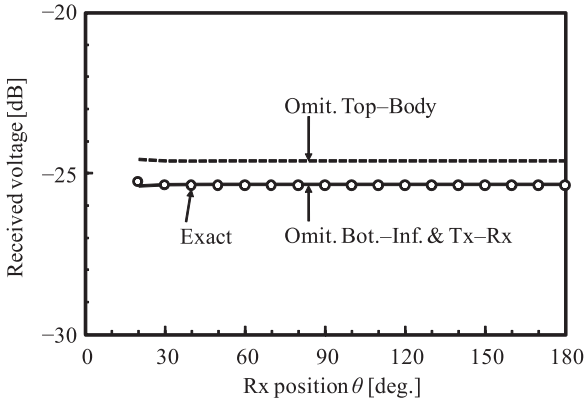

Fig. 12 Received voltages with omitting some parameters when both of the transmitter and the receiver are grounded.

ceiver are relatively small, they are omissible. Therefore, the received voltage is supposed to be independent with the equipping position of devices. Similarly, some couplings with grounded electrodes are expected to be omissible. Figures 10–12 plot the received voltages with omitting some parameters in the respective cases. The common point is that the direct couplings between the devices are almost omissible as expected (plotted with solid lines). In addition, the results indicate that the coupling between the bottom electrode of grounded device and the infinite distance is also omissible. Furthermore, even if the coupling between the grounded electrode and the human body is omitted, the discrepancy with the exact result is very small. This is also due to the same reason, that is, the capacitance of the body with the grounded electrode is sufficiently small than that with the infinite distance.

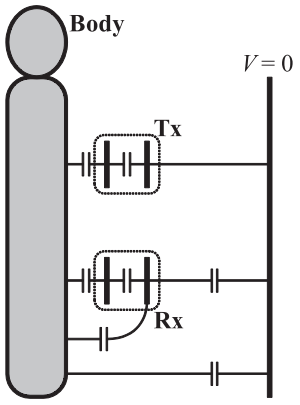

Fig. 13 Approximate model when the transmitter is grounded.

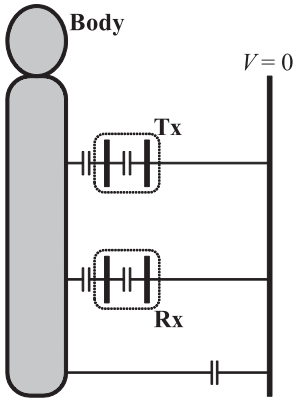

Fig. 14 Approximate model when both of the transmitter and the receiver are grounded.

Figure 13 shows the approximate model when the transmitter is grounded. This circuit model suggests not only that the channel is independent on the device positions, but also that the potential of the body is sensitive to the capacitance between the bottom electrode of the transmitter and the body. In other words, the received voltage strongly depends on the distance between the transmitter and the body. Therefore, it may be suggested that an action touching the off-body transmitter can be used as a trigger for communications. In addition, the approximate model when the receiver is grounded have a composition that the transmitter and the receiver are interchanged in Fig. 13.

Finally, Fig. 14 shows the approximate circuit model for the case that both of the transmitter and the receiver are grounded. This model is relatively similar to models pro-

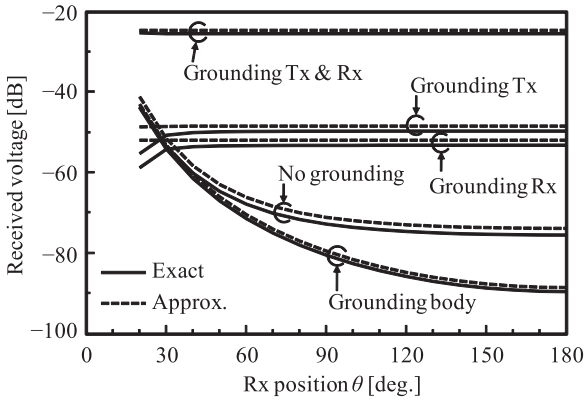

Fig. 15 Received voltages calculated by using exact and approximate models.

posed in some previous studies [7]. Of course, if we measure the channel with a network analyzer, the channel should behave as Fig. 14. Therefore, if we need to assess the channels for on-body applications, the devices should be isolated from the ground of the instruments.

5.4 Received Voltages by Using Approximate Models

In order to examine the validity of the approximate models described in previous subsections, Fig. 15 compares the received voltages calculated by using the approximate models with the exact values. In all the cases, the discrepancies are less than 2 dB in a range of $\theta \geq 40^\circ$. Hence, the approximate models proposed here are most likely enough to grasp the behavior of the channel.

6. Conclusion

In the present study, the equivalent-circuit expressions of the intra-body communications channels using the quasi-static field were properly derived by solving a boundary value problem of electric potentials of the electrodes and the human body. Then, the signal transmission characteristics in various conditions were calculated with the obtained circuit parameters. According to the results, in the case that either or both of the transmitter and the receiver are grounded, the value and the stability of the received voltage are improved because the coupling through the infinite distance becomes dominant.

Furthermore, after we have investigated omissible circuit parameters in each case, it is found that in the case that the devices are not grounded, many parameters, especially the direct couplings between the transmitter and the receiver, are not negligible. Similarly, in the case that the human body is grounded, the most of parameters should be taken into account. We believe that these facts are important in considering on-body applications such as e-healthcare and personal services. By contrast, if either of the transmitter and the receiver is grounded, the direct couplings between them are negligible. This fact is most likely important for off-body applications such as personal authentication and electronic payment. Especially, in the case that the both devices are grounded, many parameters may be omitted; and therefore, the approximate circuit model is relatively similar to models proposed in some previous studies. Of course, if we measure the channels with a network analyzer, the channel should behave as the last case. Therefore, the devices should be isolated from the ground of the instruments to correctly assess the channels for on-body applications.

In the future, we will consider some effects due to proximity of the earth ground and variations of human posture by employing more realistic human body models.

References

[1] P.S. Hall and Y. Hao, Antennas and Propagation for Body-Centric Wireless Communications, Artech House, Norwood, MA, 2006.
[2] Special Issue on "Antennas and propagation for body-centric wireless communications," IEEE Trans. Antennas Propag., vol.57, no.4, pp.833–1016, April 2009.
[3] C. Baber, T.N. Arvanitis, D.J. Haniff, and R. Buckley, "A wearable computer for paramedics: Studies in model-based, user-centred and industrial design," Proc. INTERACT 99, pp.126–132, Edinburgh, U.K., Aug.–Sept. 1999.
[4] T.G. Zimmerman, "Personal area networks: Near-field intra-body communication," IBM Syst. J., vol.35, no.3/4, pp.609–617, 1996.
[5] K. Hachisuka, Y. Terauchi, Y. Kishi, K. Sasaki, T. Hirota, H. Hosaka, K. Fujii, M. Takahashi, and K. Ito, "Simplified circuit modeling and fabrication of intrabody communication devices," Sensors and Actuators A Physical, A130–131, pp.322–330, April 2006.
[6] N. Cho, J. Yoo, S. Song, J. Lee, S. Jeon, and H. Yoo, "The human body Characteristics as a signal transmission medium for intrabody communication," IEEE Trans. Microw. Theory Tech., vol.55, no.5, pp.1080–1086, May 2007.
[7] A. Sasaki and M. Shinagawa, "Principles and demonstration of intrabody communication with a sensitive electrooptic sensor," IEEE Trans. Instrum. Meas., vol.58, no.2, pp.457–466, Feb. 2009.
[8] N. Matsushita, S. Tajima, Y. Ayatsuka, and J. Rekimoto, "Wearable key: Device for personalizing nearby environment," Proc. 4th Int. Symp. Wearable Comput., pp.119–126, 2000.
[9] K. Fujii, M. Takahashi, and K. Ito, "Electric field distributions of wearable devices using the human body as a transmission channel," IEEE Trans. Antennas Propag., vol.55, no.7, pp.2080–2087, July 2007.
[10] M. Taki, Y. Suzuki, and K. Watanabe, "Exposure assessment of a human-body communication system with electric field coupling with body," IEICE Technical Report, EMCJ2007-47, Sept. 2007. (in Japanese)
[11] N. Haga and K. Ito, "Frequency dependence of on-body channels with top-loaded monopole antennas in the range of HF to UHF," Proc. Asia-Pacific Microwave Conf. 2009, pp.2208–2211, Singapore, Dec. 2009.
[12] T. Nagaoka, S. Watanabe, K. Sakurai, E. Kunieda, S. Watanabe, M. Taki, and Y. Yamanaka, "Development of realistic high-resolution whole-body voxel models of Japanese adult male and female of average height and weight, and application of models to radio-frequency electromagnetic-field dosimetry," Phys. Med. Biol., vol.49, pp.1–15, 2004.
[13] R.F. Harrington, Field Computation by Moment Methods, The Macmillian, New York, 1968.
[14] M. Abramowitz and I.A. Stegun, Handbook of Mathematical Functions with Formulas, Graphs, and Mathematical Tables, Dover Publications, New York, 1972.
[15] A.N. Tikhonov and A.A. Samarskii, Equations of Mathematical Physics, Dover Publications, New York, 1963.
[16] A. Taflove, Advances in Computational Electrodynamics: The

Finite-Difference Time-Domain Method, Artech House, Norwood, MA, 1998.

Appendix: Applicable Frequency of Quasi-Static Approximation

The approximate circuit model in Fig. 14 implies that the received voltage decreases with frequency because the relative amount of impedance of human body increases with frequency. As an example, we assume a lossy circuit model shown in Fig. A· 1, which includes a resistance component R between two points on the human body which face each bottom electrode of the transmitter and the receiver. With this assumption, we find the received voltage V_2 for input voltage V_1 as

$$V_2 = \frac{C_2}{(C_2 + C_3)(j\omega RC_7 + 1) + C_7} \cdot \frac{C_5}{C_4 + C_5} V_1 \quad (\text{A}\cdot 1)$$

where, $C_7 = C_4C_5/(C_4 + C_5) + C_6$. Equation (A· 1) indicates that V_2 decreases with increasing ω. In order to assess the extent of this depression, we have additionally calculated the frequency characteristics of received voltage with a lossy sphere model ($\epsilon_r = 91.8$, $\sigma = 0.658$ S/m: muscle at 30 MHz) by using the FDTD method.

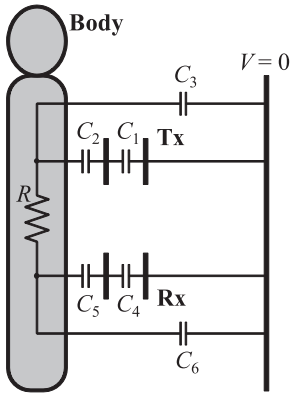

Fig. A· 1 Approximate model including a resistance component.

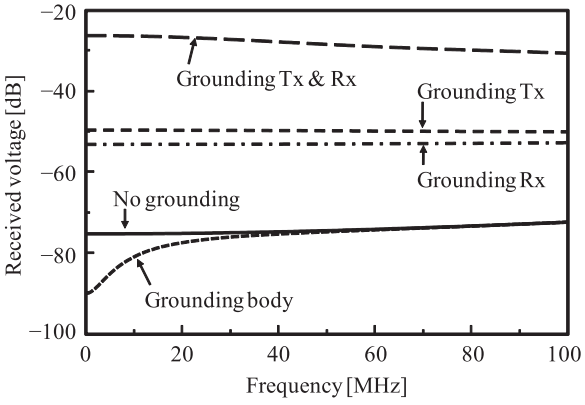

Fig. A· 2 Frequency dependence of received voltage.

Figure A· 2 plots the frequency dependence of the received voltages in respective cases. Here the position of the receiver is $\theta = 180°$. At zero frequency, the voltages almost agree with that in Fig. 4 except just a little numerical error. As implied by Eq. (A· 1), the received voltage when both devices are grounded decreases with increasing frequency. However, the depression is within 3 dB below 60 MHz. In addition, the received voltage with the grounded body approaches to that with the ungrounded body as the frequency increases. This is due to a fact that it takes relatively long time before the excited electromagnetic waves have propagated to the infinite distance through around the body and the grounding wire.

Nozomi Haga was born in Yamagata, Japan, in January 1985. He received the B.E. and M.E. degrees in electrical engineering from Chiba University, Chiba, Japan, in 2007 and 2009, respectively. He is currently working toward the D.E. degree at Chiba University. His main interests have been electrically small antennas for personal communications, and evaluation of the interaction between electromagnetic field and the human body by use of numerical and experimental phantoms.

Kazuyuki Saito was born in Nagano, Japan, in May 1973. He received the B.E., M.E. and D.E. degrees all in electronic engineering from Chiba University, Chiba, Japan, in 1996, 1998 and 2001, respectively. He is currently an Assistant Professor with the Research Center for Frontier Medical Engineering, Chiba University. His main interest is in the area of medical applications of the microwaves including the microwave hyperthermia. He received the IEICE AP-S Freshman Award, the Award for Young Scientist of URSI General Assembly, the IEEE AP-S Japan Chapter Young Engineer Award, the Young Researchers' Award of IEICE, and the International Symposium on Antennas and Propagation (ISAP) Paper Award in 1997, 1999, 2000, 2004, and 2005 respectively. Dr. Saito is a member of the Institute of Image Information and Television Engineers of Japan (ITE), and the Japanese Society for Thermal Medicine.

Masaharu Takahashi was born in Chiba, Japan, in December, 1965. He received the B.E. degree in electrical engineering in 1989 from Tohoku University, Miyagi, Japan, and the M.E. and D.E. degrees both in electrical engineering from Tokyo Institute of Technology, Tokyo, Japan, in 1991 and 1994 respectively. He was a Research Associate from 1994 to 1996, an Assistant Professor from 1996 to 2000 at Musashi Institute of Technology, Tokyo, Japan, and an Associate Professor from 2000 to 2004 at Tokyo University of Agriculture and Technology, Tokyo, Japan. He is currently an Associate Professor at the Research Center for Frontier Medical Engineering, Chiba University, Chiba, Japan. His main interests are electrically small antennas, planar array antennas, and electromagnetic compatibility. He received the IEEE Antennas and Propagation Society (IEEE AP-S) Tokyo chapter young engineer award in 1994.

Koichi Ito was born in Nagoya, Japan, in June, 1950. He received the B.S. and M.S. degrees from Chiba University, Chiba, Japan, in 1974 and 1976, respectively, and the D.E. degree from the Tokyo Institute of Technology, Tokyo, Japan, in 1985, all in electrical engineering. From 1976 to 1979, he was a Research Associate at the Tokyo Institute of Technology. From 1979 to 1989, he was a Research Associate at Chiba University. From 1989 to 1997, he was an Associate Professor at the Department of Electrical and Electronics Engineering, Chiba University, and is currently a Professor at the Graduate School of Engineering, Chiba University. He has been appointed as one of the Deputy Vice-Presidents for Research, Chiba University, since April 2005. In 1989, 1994, and 1998, he visited the University of Rennes I, France, as an Invited Professor. Since 2004 he has been appointed as an Adjunct Professor to Institute of Technology Bandung (ITB), Indonesia. His main research interests include analysis and design of printed antennas and small antennas for mobile communications, research on evaluation of the interaction between electromagnetic fields and the human body by use of numerical and experimental phantoms, microwave antennas for medical applications such as cancer treatment, and antennas for body-centric wireless communications. Dr. Ito is a member of the American Association for the Advancement of Science, the Institute of Image Information and Television Engineers of Japan (ITE) and the Japanese Society for Thermal Medicine (formerly, Japanese Society of Hyperthermic Oncology). He served as Chair of the Technical Group on Radio and Optical Transmissions, ITE from 1997 to 2001 and Chair of the Technical Group on Human Phantoms for Electromagnetics, IEICE from 1998 to 2006. He also served as Chair of the IEEE AP-S Japan Chapter from 2001 to 2002 and TPC Co-Chair of the 2006 IEEE International Workshop on Antenna Technology (iWAT2006). He currently serves as General Chair of the iWAT2008 to be held in Chiba, Japan in 2008, Vice-Chair of the 2008 International Symposium on Antennas and Propagation (ISAP2008) to be held in Taiwan in 2008 and as an Associate Editor for the IEEE TRANSACTIONS ON ANTENNAS AND PROPAGATION. He also serves as a Distinguished Lecturer and an AdCom member for the IEEE Antennas and Propagation Society since January 2007.